Available online at www.sciencedirect.com

ScienceDirect

Energy Procedia 124 (2017) 418–424

Energy Procedia

www.elsevier.com/locate/procedia

7th International Conference on Silicon Photovoltaics, SiliconPV 2017

Dependence of n-cSi/MoO_x Heterojunction Performance on cSi Doping Concentration

Hisham Nasser[a,*], Gamze Kökbudak[a], Haris Mehmood[a,b], Raşit Turan[a]

[a]*The Center for Solar Energy Research and Applications (GÜNAM), Middle East Technical University (METU), Ankara, Turkey*
[b]*National University of Sciences and Technology (NUST), Islamabad, Pakistan*

Abstract

In this work, we demonstrate a strong correlation between crystalline silicon (cSi) base doping concentration and the performance of cSi/MoO_x heterojunction solar cell by investigating the structure numerically based on Silvaco TCAD simulation tool and experimentally. The doping concentration of n-type cSi was scanned in the $1 \times 10^{15} - 2 \times 10^{16}$ cm^{-3} range. Simulation results show that utilizing highly doped cSi wafer degrades the conversion efficiency of cSi/MoO_x solar cell. Efficiency of 11.16% has been obtained from simulation results for 1×10^{15} cm^{-3} doping concentration while this value reduces to less than 4% for wafer with a doping concentration of 2×10^{16} cm^{-3}. These simulation results were demonstrated experimentally and n-type cSi wafers with two different doping concentrations were considered, 1×10^{15} and 5.5×10^{15} cm^{-3}. The key concept underlying this work is to differentiate explicitly the effect of cSi doping concentration on the performance of cSi/MoO_x cell, thus a simple cell design is considered where n-type cSi wafers were heavily phosphorous-doped to form (n^+) at the front of the Si and thermally evaporated MoO_x films with various thicknesses (<15 nm) were inserted at the rear between cSi and Al contact. In accordance to simulation results, highly doped wafer exhibited low conversion efficiency of 3.32% while using lower doped wafer significantly improves the efficiency from 3.32 to 10.9%.

Peer review by the scientific conference committee of SiliconPV 2017 under responsibility of PSE AG.

Keywords: cSi/MoO_x; Heterojunction solar cell; Schottky junction; Simulation.

* Corresponding author. Tel.: +90-312-210-5076; fax: +90-312-210-5099.
E-mail address: nasser@metu.edu.tr

1876-6102
Peer review by the scientific conference committee of SiliconPV 2017 under responsibility of PSE AG.
10.1016/j.egypro.2017.09.267

1. Introduction

Development of low cost and highly efficient crystalline silicon (cSi) solar cells are amongst the key goals guiding the PV community in order to shore up the implementation of PV technology at a greater scale worldwide. Crucial PV cost reduction approaches include employing either ultra-thin silicon (Si) wafers or low-quality substrates, nonetheless, in either case, reduced thermal budgets and simplified designs are necessary for commercial production. In this sense, designs based on Si heterojunction comprise a cornerstone in which lower fabrication temperatures and higher efficiencies can be merged [1]. Yet, the p- and n-doped thin a-Si:H layers commonly used for Si heterojunction solar cells are usually deposited by a capital-intensive PECVD tool using hazardous gases in addition to the toxic by-products generated. Consequently, employing risk-free layers further reducing the fundamental limitations and fabrication costs are highly desirable. These layers are basically transition metal oxides (TMO) and alkali metal fluorides (AMF) which act as an efficient hole and electron selective contacts, respectively. Coupled with the high work-function of ~6.7 eV and the large band gap of ~3.3 eV, thin layers of MoO_x have already been investigated and integrated to cSi based solar cells [2-4]. Heterojunction cells based on n-cSi and MoO_x with an intrinsic a-Si:H passivation layer, have been reported demonstrating an efficiency of 18.8% [3]. Designs employing both electron and hole selective heterocontacts in cSi designs have also been reported attaining an efficiency of 15.4% in which both MoO_x and LiF layers are placed at the rear of cSi [4]. The champion dopant free cSi solar cell with efficiency of 19.42% has been fabricated by placing MoO_x and LiF layer on either side of cSi [2]. To our knowledge, however, the behaviour of MoO_x/cSi solar cell as a function of cSi doping concentration is yet to be discussed in literature explicitly. Motivated by this, we compare the performance of n-type cSi/MoO_x heterojunction for different cSi doping concentrations by simulations via Silvaco TCAD tool and experimental results.

2. Physical device modeling

An industrial semiconductor device simulator, Silvaco TCAD, has been used for analytically investigating the characterization behavior of the proposed PV structure. Key benefits for employing such simulator in the research setup include: (a) Realistic performance predictions of the PV device under investigation; (b) enhanced physical insight of the device; and (c) cutting down the development cost and time involved in experimental optimization of the device.

The proposed solar cell comprises 150 μm thick n-type cSi wafer with different doping concentrations, along with a thin layer of heavily n^+-doped cSi at the front side of the wafer and MoO_x at the rear, as shown in Fig. 1. The cSi base doping was varied in the range of $1 \times 10^{15} – 2 \times 10^{16}$ cm^{-3}. Following assumptions were also considered for simulation purpose: (a) thermionic emission tunnelling for transport of charge carriers at n-cSi/MoO_x interface [5-7]; (b) surface recombination velocity of 10^5 cm/s at the front and the rear; and (c) planar surface with 19% reflection of incident light from the front surface. Relevant basic material parameters for the proposed structure have been tabulated in Table 1. MoO_x layer has been assumed as a contact layer in our simulation and also reported as a contact layer according to the work done by Chuang *et al*. [5]. The corresponding MoO_x electrical resistivity in the range of 1×10^5-2×10^6 Ω·cm was assigned, which is in agreement with our earlier reported work [8]. Optical constants and the band gap of MoO_x thin film were obtained from the spectroscopic ellipsometry analysis (SOPRA SEA) of 15 nm film deposited on a polished silicon wafer. Various mathematical commands have been invoked with the MODELS statement that include SRH recombination (SRH), Auger recombination (AUGER), band gap narrowing effects (BGN), concentration-dependent SRH recombination (CONSRH), Fermi-Dirac statistics model (FERMI) and optical recombination (OPTR) models. All measurements were performed at a simulated temperature of 25^0C under the standard value of air mass (AM) 1.5G spectrum.

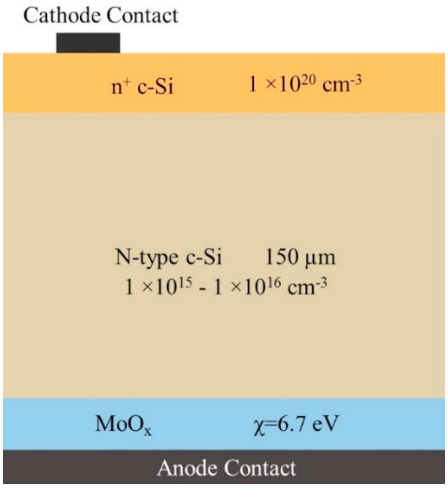

Fig. 1. Proposed solar cell design based on MoO_x layer utilized in Silvaco TCAD device simulator.

3. Simulated results and discussion

It is essential to reliably simulate the structure by incorporating all relevant parameters for cSi and MoO_x layer that can affect the overall PV performance. Fig. 2 illustrates the effect of base doping concentration on the PV performance of the proposed structure shown in Fig. 1. It can be observed that for the simulated range of n-cSi doping concentration, V_{oc} reduces slightly from 0.58 V to around 0.57 V. However, large degradation in J_{sc} with a corresponding increase in cSi doping concentration can be attributed to the reduction in Schottky barrier width at conduction band edges between n-cSi and MoO_x layer. The depletion region within n-cSi becomes thinner with elevated doping levels that allow tunnelling of electrons through n-cSi/MoO_x interface to reach the anode region. As a result, these tunnelled electrons reduce the hole-selectivity of MoO_x and correspondingly, the power conversion efficiency (PCE) of the solar cell deteriorates quite significantly as well. The proposed device numerically achieved the V_{oc} of 578.9 mV, J_{sc} of 29.6 mA/cm^2, *FF* of 65%, and PCE (η) of 11.16% with 15 nm thick MoO_x . Though these

Table 1. Input Silvaco TCAD Parameters for different layers.

Parameters	*n*-cSi	n^+-cSi	*Front interface*	*Rear interface*
Electron affinity χ (eV)	4.17	4.17	-	-
Permittivity ε_r (eV)	11.7	11.7	-	-
Energy band gap E_g (eV)	Doping dependent	1.12	-	-
Interface recombination velocity (cm/s)	-	-	1×10^5	1×10^5
Effective DOS in conduction band N_C (cm^{-3})	2.77×10^{19}	2.77×10^{19}	-	-
Effective DOS in valence band N_V (cm^{-3})	1.03×10^{19}	1.03×10^{19}	-	-
SRH Electron lifetime τ_n (sec)	1×10^{-4}	1×10^{-4}	-	-
SRH Hole lifetime τ_p (sec)	1×10^{-3}	1×10^{-3}	-	-
SRH concentration for electrons N_{SRHn} (cm^{-3})	5×10^{16}	5×10^{16}	-	-
SRH concentration for holes N_{SRHp} (cm^{-3})	5×10^{16}	5×10^{16}	-	-
Trap energy for SRH recombination E_{trap} (eV)	0	0	-	-
Electron Auger coefficient C_n (cm^6/s)	2.8×10^{-31}	2.8×10^{-31}	-	-
Hole Auger coefficient C_p (cm^6/s)	9.9×10^{-32}	9.9×10^{-32}	-	-
Optical recombination rate C_{opt} (cm^3/s)	1.1×10^{-14}	1.1×10^{-14}	-	-

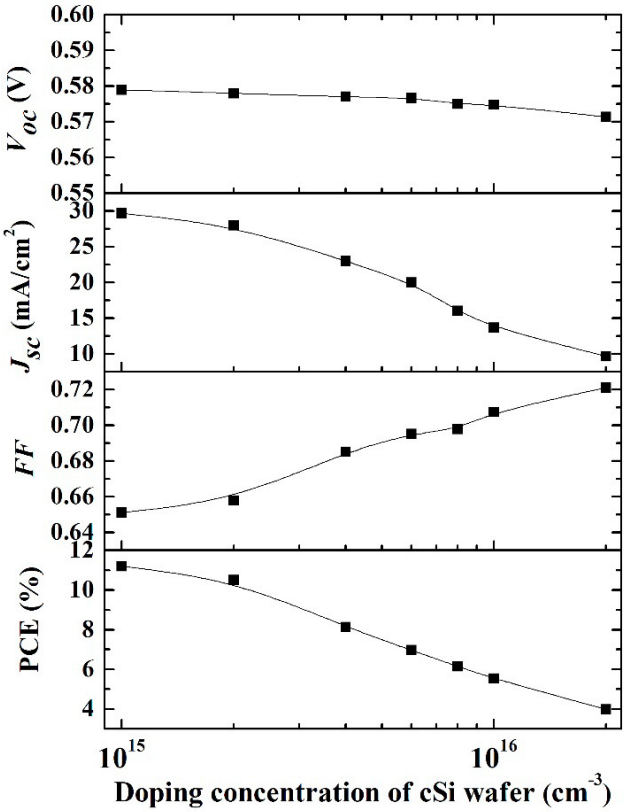

Fig. 2. Simulated PV characterization of n-type cSi/MoO_x with 15 nm thick MoO_x at different doping concentrations.

simulated results are in good approximation with the experimental work presented in this paper, still, the efficiency is low due to the absence of cSi passivation as well as antireflection coating (ARC) layers. With the inclusion of intrinsic a-Si:H as a passivation layer, enhanced values of V_{oc} can be expected due to the reduced interface recombination velocity.

4. Fabrication of MoO_x/cSi heterojunction solar cell

Solar cells were fabricated on front-side pyramidal textured in potassium hydroxide (KOH) solution, FZ, n-type cSi wafers with the thickness of ~150 µm. Set of cSi wafers with two different doping concentrations were considered, 1×10^{15} cm^{-3} and 5.5×10^{15} cm^{-3}. Following standard RCA cleaning and a dilute hydrofluoric acid (HF) dip, heavily doped region (n^+) was formed at the front of the Si wafers via thermal doping while applying SiN_x diffusion mask at the rear side, to create the desired ohmic contact between the Si surface and the front electrode. Right after removal of the native oxide in dilute HF and SiN_x rear diffusion mask, MoO_x thin films with two different thicknesses of 10 and 15 nm were thermally evaporated onto the rear of n-type cSi wafers from stoichiometric MoO_3 powder (>3N purity) at a deposition rate of 0.2 Å/s (as monitored by a crystal oscillator) at a pressure of 4×10^{-6} mbar. Finally, full coverage Al rear contact and Al front grids (~5% coverage) were thermally evaporated (Fig. 3a). The proposed cell design in this work allows a discrete perceiving of cSi doping concentration impact on MoO_x capacity to contact holes selectively since this design eliminates undesirable contributions and optical based losses from different layers often used in cSi/MoO_x designs such as the passivation layer and the TCO usually associated with MoO_x layer placed at the cell front surface. A set of reference solar cell samples without MoO_x layer were also fabricated (Fig. 3b).

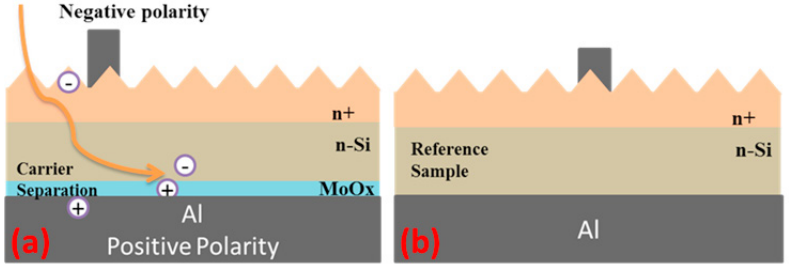

Fig. 3. Conceptual schematics of (a) n-cSi/MoO_x heterojunction; (b) reference solar cell without MoO_x.

5. Results and discussion

Simulation results reveal that employing lightly doped cSi wafer results in higher conversion efficiency up to 11.16% from n-cSi/MoO_x heterojunction solar cell with 15 nm thick MoO_x layer and 1×10^{15} cm^{-3} doping concentration (Fig. 2). Similar behaviour is observed from the fabricated n-cSi/MoO_x heterojunction solar cells (Fig. 4a). This behaviour was observed because when a material with a very high work function such as MoO_x is applied to lightly doped cSi, accumulation of holes and repulsion of electrons occurs at the surface. This high hole concentration at the surface reduces the heterocontact resistivity while the corresponding low electron concentration at the surface reduces the probability of Shockley-Read-Hall recombination at the heterocontact interface. With increasing the n-cSi doping concentration, the PV performance degraded (Fig. 2 and Fig 4b). The current density−voltage (J−V) curves of the MoO_x/Si solar cells thickness were analyzed under AM 1.5G illumination. The V_{oc}, J_{sc} (corrected from EQE measurement, Fig. 4c), *FF*, and η are summarized in Table 2.

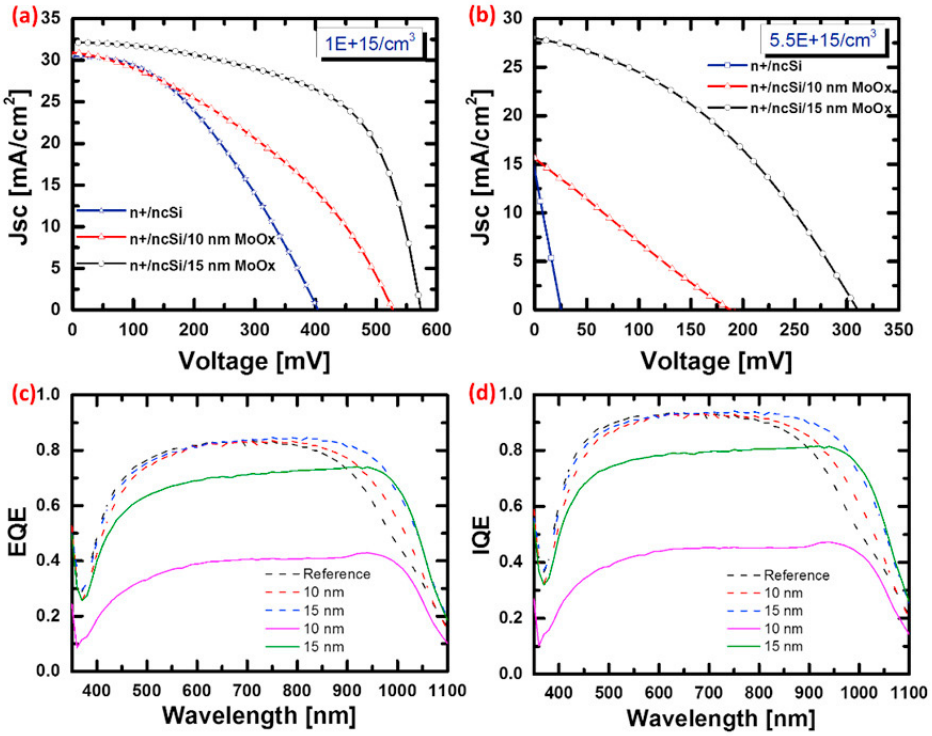

Fig. 4. (a) and (b) J-V behaviour of n-type cSi/MoO_x with 1×10^{15} cm^{-3} and 5.5×10^{15} cm^{-3} doping concentration, respectively; (c) and (d) measured EQE and calculated IQE; respectively, of the fabricated devices with 1×10^{15} cm^{-3} (dashed lines) and 5.5×10^{15} cm^{-3} (solid lines).

For a lightly doped cSi, MoO_x-layer-free device exhibited a very low conversion efficiency of 4.89% along with low V_{oc} of 403.9 mV. This result was obtained because the Si/Al Schottky junction did not effectively separate the photogenerated carriers, as a result of the high defect density at Al/Si interface. On the other hand, placing MoO_x layer between Al and Si improved the efficiency from 4.88 to 10.89% for 15 nm thick MoO_x layer. As 10 nm thick MoO_x cannot fully cover the Si surface, the efficiency slightly increased from 4.88% to 6.23% since direct Al-Si local contact Schottky junction reduces the desired diode property of the Si/MoO_x junction. The result of 10 nm thick MoO_x contradicts the simulation results which showed that the 10 nm thick MoO_x leads to the highest η of 11.2%, with V_{oc} of 578.9 mV, J_{sc} of 29.7 mA/cm^2, and *FF* of 65.1%. This suggests that there exist some local areas on cSi surface which are not covered by the MoO_x. It is worth mentioning that there are several prospective routes to boost the cell performance; which is not within the scope of this study. V_{oc} can be improved by including a passivation layer on either side of the wafer. A higher J_{sc} could be achieved by adding an antireflection coating layer. For instance, J_{sc} of 36.15 mA/cm^2 calculated from IQE data (Fig. 4d) increases the efficiency from 10.89% to 12.33% for cell with 15 nm thick MoO_x layer as shown in Table 2. Finally, *FF* can be improved by adjusting the defect states in MoO_x and having ultra-thin yet conformal deposited MoO_x film. In addition, series resistance which is relatively high as shown in Table 2 can be reduced by optimizing the contact geometry.

For a highly doped wafer, device without MoO_x did not show any diode behaviour, because increasing cSi doping concentration results in a thin depletion layer width between Al and Si. As a result, photogenerated carriers can tunnel across the barrier leading to a rather ohmic behaviour. Placing MoO_x between Si and Al formed a diode (between MoO_x and cSi) with a slightly improved efficiency of up to 3.32% was observed for 15 nm thick MoO_x layer.

The degraded PV performance with increasing cSi doping concentration suggests that the transport mechanism in n-cSi/MoO_x junction is governed by thermionic emission of majority carriers over the Schottky barrier at n-cSi/MoO_x interface and not by diffusion of minority charge carriers. With increasing n-cSi doping concentration, the Schottky barrier width for conduction band edges between MoO_x and n-cSi reduces drastically allowing electrons to tunnel through by the application of electric field and reach to the Al contact which lessens the hole selective capacity of MoO_x and thus deteriorating the solar cell performance overall.

Table 2. Solar cell photovoltaic performance of n-cSi/MoO_x

Doping (cm^{-3})	MoO_x Thickness (nm)	V_{oc} (mV)	J_{sc} (mA/cm^2)	J_{sc} *(IQE)* *(mA/cm^2)*	*Rsh* (Ω.cm^2)	*Rs* (Ω.cm^2)	*FF* (%)	η (%)	η *(IQE)* (%)
	0 (Reference)	403.9	30.3	34.30	180.61	6.75	39.9	4.88	5.53
1×10^{15}	10	526.8	30.6	34.64	135.94	6.71	38.6	6.23	7.05
	15	572.6	31.9	36.15	367.35	2.15	59.6	10.89	12.33
	0	25.3	NA	NA	NA	NA	NA	NA	NA
5.5×10^{15}	10	188.0	15.5	17.6	12.07	13.1	24.1	0.70	0.80
	15	310.4	28.0	31.8	75.21	5.74	38.2	3.32	3.78

6. Conclusion

In this paper, we have combined simulated results based on Silvaco TCAD simulation tool and experimental findings of n-cSi/MoO_x solar cell to identify the nature of the heterojunction formed between cSi and MoO_x hole selective layer. Our results show that utilizing lightly doped n-cSi wafer is a prerequisite to attain high conversion efficiencies from n-cSi/MoO_x heterojunction solar cell. Fabricated n-cSi/MoO_x heterojunction solar; with 1×10^{15} cm^{-3} doping concentration and 15 nm thick MoO_x hole transport layer, show high efficiency of almost 11% and open circuit voltage of up to 573 mV even for a simple structure without passivation and antireflection coating layers, or optimized contact. According to the presented work, we clearly show that MoO_x forms a hybrid heterojunction with n-cSi behaving as Schottky junction and not like a conventional pn-junction in which conversion efficiency is expected to increase with increasing doping concentration up to certain level.

Acknowledgements

Haris Mehmood would like to thank Scientific and Technological Research Council of Turkey (TÜBİTAK), for providing research grant under 2216 - Research Fellowship Programme for International Researchers, No. 21514107-115.02-5631.

References

[1] Masuko K, Shigematsu M, Hashiguchi T, Fujishima D, Kai M, Yoshimura N, et al. Achievement of More Than 25% Conversion Efficiency With Crystalline Silicon Heterojunction Solar Cell. IEEE Journal of Photovoltaics 2014; 4(6):1433–1435.

[2] Bullock J, Hettick M, Geissbühler J, Ong AJ, Allen T, Sutter-Fella CM, et al. Efficient silicon solar cells with dopant-free asymmetric heterocontacts. Nat Energy 2016;1:15031. Available from: http://dx.doi.org/10.1038/nenergy.2015.31

[3] Battaglia C, de Nicolás SM, De Wolf S, Yin X, Zheng M, Ballif C, et al. Silicon heterojunction solar cell with passivated hole selective MoOx contact. Appl Phys Lett 2014;104(11):113902. Available from: http://dx.doi.org/10.1063/1.4868880

[4] Um H-D, Kim N, Lee K, Hwang I, Seo JH, Seo K. Dopant-Free All-Back-Contact Si Nanohole Solar Cells Using MoOx and LiF Films. Nano Lett 2016;16(2):981–987. Available from: http://dx.doi.org/10.1021/acs.nanolett.5b03955

[5] Chuang S, Battaglia C, Azcatl A, McDonnell S, Kang JS, Yin X, et al. MoS(2) P-type transistors and diodes enabled by high work function MoOx contacts. Nano Lett. 2014;14(3):1337–1342.

[6] Meyer J, Hamwi S, Kröger M, Kowalsky W, Riedl T, Kahn A. Transition Metal Oxides for Organic Electronics: Energetics, Device Physics and Applications. Adv Mater 2012;24(40):5408–5427. Available from: http://dx.doi.org/10.1002/adma.201201630

[7] Stradins P, Essig S, Nemeth W, Lee BG, Young D, Norman A, et al. Passivated Tunneling Contacts to N-Type Wafer Silicon and Their Implementation into High Performance Solar Cells: Preprint. WCPEC-6: 6th World Conference on Photovoltaic Energy Conversion Japan 2014. Available from: http://www.osti.gov/scitech/servlets/purl/1166658

[8] Ahiboz D, Nasser H, Turan R. Admittance Analysis of Thermally Evaporated-Hole Selective MoO_3 on Crystalline Silicon. 4th International Renewable and Sustainable Energy Conference (IRSEC'16). Marrakech, Morocco 2016; p. In press, IEEE Xplore.